


Zakariya Zubair<sup>1,2,\*</sup>   
Moussa Alali<sup>1,2</sup>  
Gildas L'hostis<sup>1,2</sup>  
Muhammad Zubair<sup>3</sup>  
Jean-Yves Drean<sup>1,2</sup>

# Development of Multilayer Woven Fabrics for the Adoptive Geometry Composite Structure

DOI: 10.5604/01.3001.0014.6384

<sup>1</sup> Université de Haute Alsace,  
LPMT EA 4365, F-68100 Mulhouse, France,  
\* e-mail: engrzakariya@gmail.com

<sup>2</sup> Université de Strasbourg,  
France

<sup>3</sup> National Textile University,  
Faisalabad, Pakistan

## Abstract

*In this study nine multilayer 3D woven structures were produced using polyamide filament yarns both in the warp and weft direction. Three different weaves: plain, 1/3 twill and 3/1 rib in the middle layer, and plain weave in both the top and bottom layers were produced. All specimens were developed on a narrow weaving machine equipped with multi beams and creel options. The samples were tested for tensile strength, air permeability, compressibility, resilience, bending and shear stiffness. Better compressibility was observed in 3/1 warp rib, followed by 1/3 twill and plain weave in the middle layer. Shear stiffness and bending rigidity were higher for those fabrics which had a plain weave in all layers and higher filling density. The air permeability was higher for low weft density, plain weave and its derivative 3/1 warp rib in the middle layer. Tensile strength was higher for those fabrics which were produced with higher weft densities.*

**Key words:** 3D multilayer fabric, polyimide filament yarns, shearing stiffness, compressibility, resilience.

Many researches have been conducted to study the effects that various reinforcements have upon the shape memory characteristics of polymer composites [3]. It is believed that reinforcement comprises of long fibres demonstrate better reinforcing ability than its short-fibre or particle counterparts [4-5]. In fact, long-fibre reinforced SMP composites, unlike their counterparts (particle or short-fibre), always remain more advantageous due to their high stiffness, good strength, and other remarkable mechanical characteristics [6]. However, in the recent era, researchers have significantly investigated an emerging class of reinforcement, namely 3D woven fabrics. A considerable amount of attention is being given to these fabrics because of industry's requirement for fewer steps performed, improved thickness and other mechanical properties. For instance, enhancing the delamination resistance, interlaminar-shear strength and impact damage tolerance is immensely important in the structural design procedure, which was previously missing in 2D woven fabrics reinforcements [7-8].

Multilayer 3D woven fabrics as composite preforms have an important role in the development of advanced textile composites for high performance applications. 3D woven fabrics can be manufactured by conventional weaving machines and by specially designed weaving machines. By studying the configuration and geometry of 3D woven fabrics, they can be classified by different techniques, that is, solid, hollow, shell, and nodal [9-11].

The most important type which is used as a preform in 3D composites is 3D solid woven fabric. These fabrics are manufactured by incorporating and manipulating yarns in the length, width, and through-the-thickness directions. The employment of through-the-thickness yarn within the architecture differs greatly depending upon the end use application of the preform. Through-the-thickness yarn is incorporated at varying levels and angles within orthogonal, angle-interlock, and multilayer woven architectures to obtain the desired mechanical properties, such as resistance against delamination and impact damage [10].

For multilayer woven structures, widely used 3D techniques are employed; hence, the study of these structures is very significant. The impact resistance and delamination toughness properties of 3D woven composites have been analysed by various researchers [12-14]. Similarly, the tensile, compressive, and flexural behaviour of 3D woven composites has been studied comprehensively [14-16].

Compaction of the reinforcement during composite formation affects its permeability. While the permeability of preforms is mainly determined by gaps or channels between fibre tows [17]. The inter-tow voids or resin channels in the stack of multilayer woven structures also depend upon their structure and type of input material. Grujicic et al. adopted a lubrication model to study the effect of compaction pressure, fabric-tow shearing and fabric layer shifting on the per-

## Introduction

In the present era, polymer-based shape memory actuators have received intensive interest because of their smart properties, especially as actuators, sensors and biomedical devices [1]. They have the ability of attaining a temporary shape and later of returning to the original shape upon a certain stimulus, such as light, heat, chemicals and a magnetic field. SMP composites are categorised into three areas depending upon the kind of reinforcement used. These are named as nano-fibre, short-fibre, particle and continuous fibre reinforced composites [2].

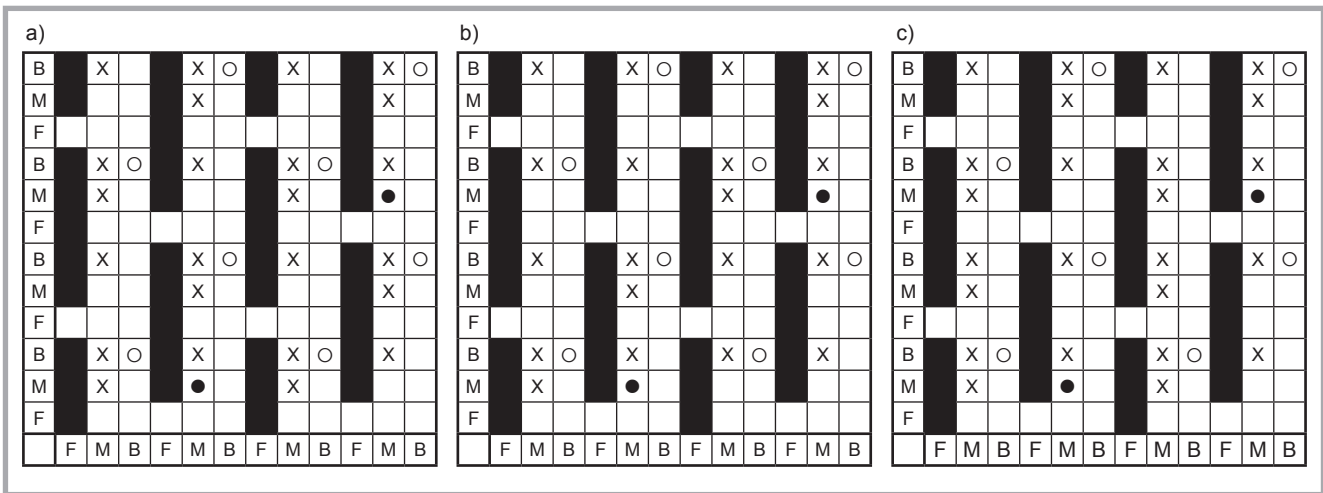


**Figure 1.** Weave design for fabric categories A, B and C (a, b and c): [x = warp of middle layer up, o = warp of back layer up, ● = stitching of warp, ■ = face layer warp up, blank square = weft yarn up].

meability of reinforcements [18]. However, more data are required to further understand the behaviour of 3D woven preforms with various multilayer weave architectures and yarns.

The aim of this study was to produce different multilayer reinforcements with three different weaves and densities using high performance polyimide filament yarn in both directions and to analyse their air permeability, bending, compression, shear and tensile properties in order to gain a better understanding of the effect of the structural properties of woven preforms which can be used as a deployable shape memory polymer composites structure.

## Material and method

### Materials

A polymer which contains repeating units linked by amide bonds is known as polyamide. Polyamides exist both artificially and naturally. Artificial polyamides (nylons, aramids, and sodium poly-aspartate) are produced by solid-phase synthesis or step-growth polymerisation, while naturally occurring polyamides are proteins (silk and wool). 100% filament nylon polyamide yarn was used in the warp and weft direction to produce three-layer interlock woven fabrics on a narrow weaving machine. Three sets of multilayer woven fabrics of 3-layers each were produced with a combination of three weaves: plain (1/1), twill (1/3) and 3/1 warp rib in the middle layer. In category G<sub>1</sub> of samples, the weave in all three layers was plain, while in groups G<sub>2</sub>

**Table 1.** Specifications of 3D-multilayer woven fabrics.

Group	Sample	Weave	Yarn linear density, tex		Warp density		Weft density, cm <sup>-1</sup>	Width, cm
			Warp	Weft	Ends, cm/layer	Ends, cm/3 layers		
G <sub>1</sub>	A1 16	Plain (1/1) weave in all layers	94	94	8	24	16	33
	A2 20		94	94	8	24	20	33
	A3 24		94	94	8	24	24	33
G <sub>2</sub>	B1 16	Face and back plain & 1/3 twill in middle	94	94	8	24	16	33
	B2 20		94	94	8	24	20	33
	B3 24		94	94	8	24	24	33
G <sub>3</sub>	C1 16	Face and back plain & 3/1 warp rib in middle	94	94	8	24	16	33
	C2 20		94	94	8	24	20	33
	C3 24		94	94	8	24	24	33

**Table 2.** Specifications of Muller NCE weaving machine.

Sr. #	Parameter	Specification/type
1.	Machine make, model and type	MULLER NCE10
2.	Machine working width (cms)	33
3.	Reed count (dents/cm)	19
4.	Speed of machine (rpm)	650
5.	Shedding type	Dobby
6.	Weft insertion type	Rapier
7.	Creel capacity	792 ends

**Table 3.** Parameters of 3D multilayer woven fabrics. **Note:** \* Values in parenthesis represent the coefficient of variation.

Samples	Crimp, %		Areal density, gm/m <sup>2</sup>		Fabric thickness, mm
	Warp	Weft	Act.	Cal.	
A1 16	2.2 (0.31)	1.7(0.57)	404.42 (1.14)	400.86	1.125 (3.39)
A2 20	2.2 (0.35)	2.7(0.39)	449.42 (0.86)	442.01	1.272 (3.98)
A3 24	2.3 (0.42)	3.3(0.50)	496.89 (1.28)	483.24	1.264 (3.81)
B1 16	1.8 (0.30)	1.1(0.52)	402.18 (1.25)	398.98	1.227 (3.10)
B2 20	2.1 (0.35)	2.4(0.64)	444.95 (0.92)	441.19	1.235 (3.52)
B3 24	1.6 (0.44)	2.8(0.73)	490.58(1.06)	480.81	1.315 (2.54)
C1 16	2.5 (1.03)	2.1(0.44)	404.45 (0.72)	402.2	1.437 (2.22)
C2 20	3.2(0.83)	2.8(0.49)	450.19 (1.90)	444.59	1.441 (3.26)
C3 24	3.3(1.27)	3.2(0.57)	489.24(1.33)	485.39	1.451 (2.31)

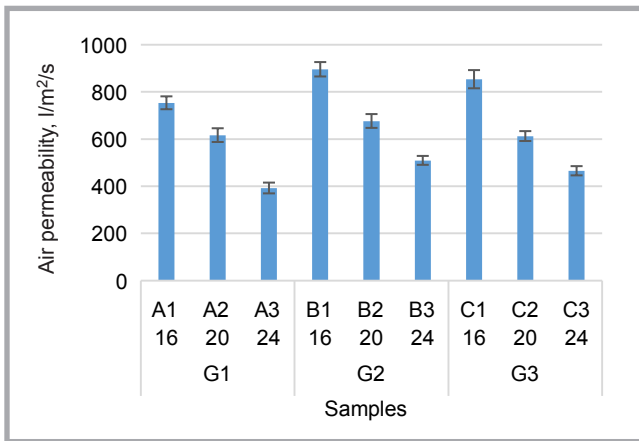


Figure 2. Air permeability of multilayer fabrics.

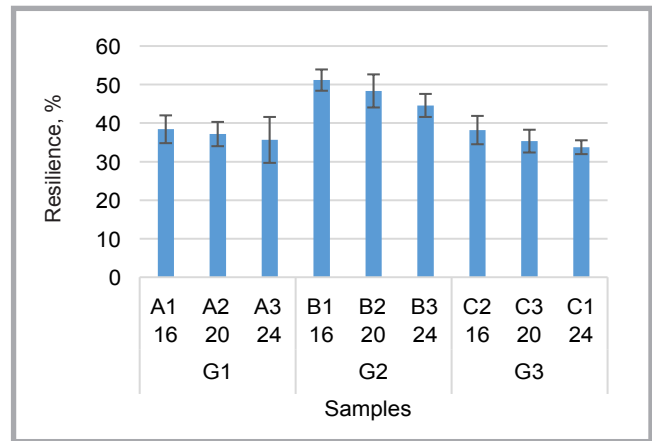


Figure 3. Effect of multilayer structure on fabric resilience.

and G<sub>3</sub> the weaves on the face and back were plain and in the middle layers 1/3 twill and 3/1 warp rib, respectively. Specifications of the multilayer woven fabrics are given in **Table 1**.

All fabric specimens were produced on a Muller NCE weaving machine. Specifications of the production machines used to manufacture the multilayer woven fabric samples are given in **Table 2**.

The weave structure used for each category of multilayer fabric is shown in **Figure 1**.

The following characteristic fabric parameters: fabric crimp, weight and thickness were measured according to test method ASTM D3883, ASTM D3776 and ASTM D1777, respectively. The mean of five values for each parameter is recorded in **Table 3**.

## Results and discussion

All the specimens were tested for air permeability, resilience, compression, bending stiffness, shear stiffness and tensile strength according to standard procedures. The mean of five values for each output variable with their coefficient of variation is recorded in **Table 4**.

### Effect of structure on air permeability

The air permeability was measured according to standard procedure NF G 07-111. The mean value of air permeability of five samples is shown in **Figure 2**. It is evident from **Figure 2** and **Table 5**, showing  $P \leq 0.05$ , that the pick density and weave structure both have a significant effect on air permeability.

All specimens in group G<sub>2</sub> exhibited higher air permeability as compared with groups G<sub>1</sub> and G<sub>3</sub>, which might be the

result of the longer diagonal float in 1/3 twill weave in the middle layer. It can also be attributed to more gaps among the yarns, which can ultimately allow a higher amount of air passage through the fabric.

Higher air permeability was observed in fabric samples woven with low pick densities (A<sub>1</sub>, B<sub>1</sub> and C<sub>1</sub>) as compared with those woven with higher weft densities because of more air passage per unit area in the lower weft density specimens.

### Effect of structure on resilience

The KES-FB3 module of Kawabata was used to measure the resilience of the fabric samples. Each woven multilayer specimen was tested five times under a standard pressure of 500 Pascal. The mean of five readings for the resilience of the multilayer fabrics is shown in **Figure 3** and **Table 4**.

Table 4. Mechanical characterisation of 3D multilayer woven fabrics. Note: \* Values in parenthesis represent the coefficient of variation.

Samples	Air permeability, l/m <sup>2</sup> /s	Resilience, %	Compressibility, %	Shear stiffness		Bending stiffness, $\mu$ N.m		Bending modulus, MPa		Tensile strength, kN	
				Warp	Weft	Warp	Weft	Warp	Weft	Warp	Weft
A1 16	753 (3.63)	38.39 (9.38)	22.75 (9.31)	0.422 (5.09)	0.406 (6.79)	383.5 (2.34)	353.04 (2.59)	3.233	2.975	13.2 (1.5)	10.4 (1.7)
A2 20	616 (4.72)	37.15 (8.47)	21.35 (13.24)	0.609 (2.5)	0.596 (3.73)	635.01 (2.46)	587.33 (2.85)	3.703	3.425	13.4 (2.5)	13.9 (1.5)
A3 24	392 (5.82)	35.63 (16.7)	17.39 (12.9)	0.843 (1.59)	0.808 (4.08)	1047.7 (2.99)	891.13 (2.4)	6.226	5.295	12.6 (2.5)	15.5 (2.3)
B1 16	895 (3.41)	51.14 (5.40)	22.93 (8.35)	0.384 (3.06)	0.384 (3.06)	326.4 (3.87)	416.5 (3.8)	2.12	2.706	12.1 (3.4)	10.4 (2.1)
B2 20	676 (4.33)	48.33 (8.88)	19.73 (11.44)	0.511 (3.12)	0.498 (6.19)	539.06 (2.8)	468.98 (2.89)	3.434	2.988	12.2 (2.8)	11.9 (6.5)
B3 24	509 (3.71)	44.57 (6.70)	18.72 (8.41)	0.631 (4.26)	0.605 (2.49)	739.9 (4.74)	620.4 (3.0)	3.905	3.274	12.8 (2.9)	13.7 (5.2)
C1 16	853 (4.52)	38.18 (9.62)	26.89 (5.56)	0.377 (3.55)	0.381 (2.89)	236.4 (4.65)	351.2 (7.3)	0.956	1.42	12.2 (1.9)	10 (3.2)
C2 20	612 (3.43)	35.32 (8.36)	24.69 (8.68)	0.473 (4.57)	0.464 (4.45)	417.07 (3.45)	617.9 (3.17)	1.673	2.478	11.7 (3.2)	12.5 (2)
C3 24	465 (4.20)	33.74 (5.31)	21.29 (6.52)	0.605 (3.18)	0.619 (4.2)	648.5 (3.14)	670.9 (2.28)	2.553	2.641	11.8 (2.9)	15.3 (0.9)

It is evident from **Figure 3** and **Table 6**, showing  $P \leq 0.05$ , that the weave structure and weft density both have a significant effect on the resilience of multilayer hybrid woven fabrics. The 1/3 twill weave in the middle layer possesses higher resilience as compared with the plain and 3/1 rib weaves, which might be due to the diagonal floats in the 1/3 twill weave of such fabrics.

Samples A<sub>1</sub>, B<sub>1</sub> and C<sub>1</sub>, produced with low pick density, presented higher resilience among the three categories – G<sub>1</sub>, G<sub>2</sub> and G<sub>3</sub>. A higher value of compressibility was found in 3-layer woven fabric produced from 1/3 twill weave in the middle layer, which might be again owing to the longer diagonal float in the warp direction.

### Effect of structure on compressibility

The KES-FB3 module of Kawabata was used to measure the compressibility of the fabric samples. The mean compression percentage of five specimens is shown in **Figure 4** and **Table 2**.

It is evident from **Figure 4** and **Table 7**, showing  $P \leq 0.05$ , that the weave structure and weft density both have a significant effect on the compressibility of the multilayer fabrics.

The multilayer fabrics produced with 1/3 warp rib in the middle layer presented higher compressibility as compared with the plain and 1/3 twill weaves, which might be attributed to the longer unidirectional floats in those fabrics. Low pick density resulted in higher compressibility among the three categories – G<sub>1</sub>, G<sub>2</sub> and G<sub>3</sub>.

### Effect of structure on bending stiffness and modulus

The cantilever or sliding test method [19], developed by Peirce [20] in 1930,

**Figure 4.** Effect of multilayer structure on fabric compressibility.

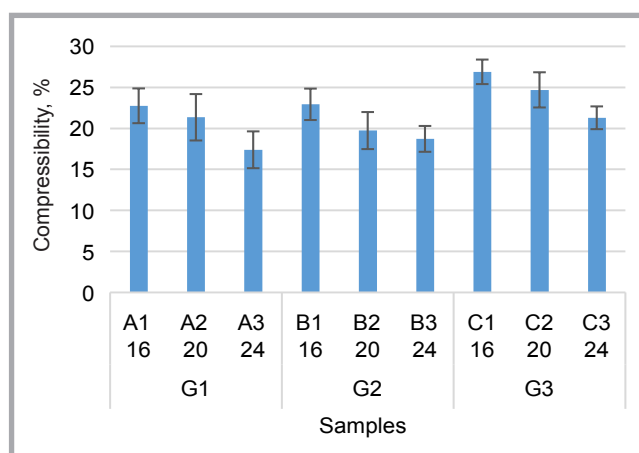


**Table 5.** Analysis of variance for air permeability.

Source	DF	Adj SS	Adj MS	F-value	P-value
Fabric	2	31928	15964	210.05	0.00
Error	6	456	76		
Total	8	32384			

**Table 6.** Analysis of variance for resilience.

Source	DF	Adj SS	Adj MS	F-value	P-value
Fabric	8	195.06	24.507	6.94	0.000
Error	18	63.54	3.53		
Total	26	259.59			

**Table 7.** Analysis of variance for compressibility.

Source	DF	Adj SS	Adj MS	F-value	P-value
Fabric	2	328.35	162.18	11.84	0.008
Error	6	82.16	13.69		
Total	8	406.51			

was used to evaluate bending stiffness  $B$  ( $\mu\text{N}\cdot\text{m}$ ). The bending stiffness  $B$  can be calculated as follows

$$B = w c^3 \quad (1)$$

Where,  $w$  is the weight per unit area and  $c = L/2$  ( $L$  – bending length). The bending modulus  $E$ , Pa [21-22] can be calculated as

$$E = \frac{12 B}{h^3} \quad (2)$$

Where,  $B$  is the bending stiffness and  $h$  the thickness of the fabric, m.

Due to the smaller width of the specimens, it was not possible to use a laboratory flex meter, therefore we had to de-

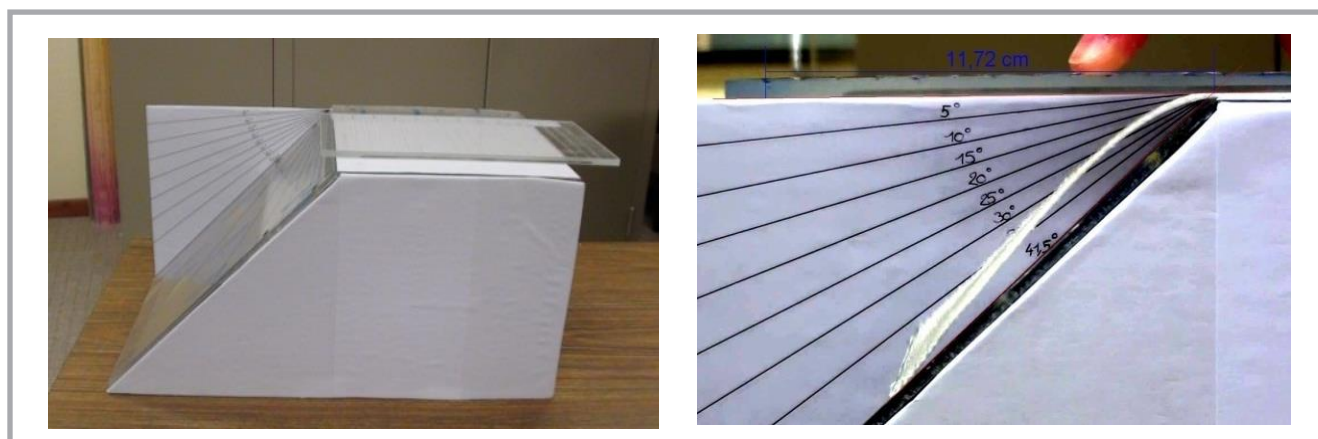


**Figure 5.** Flexo meter manufactured.

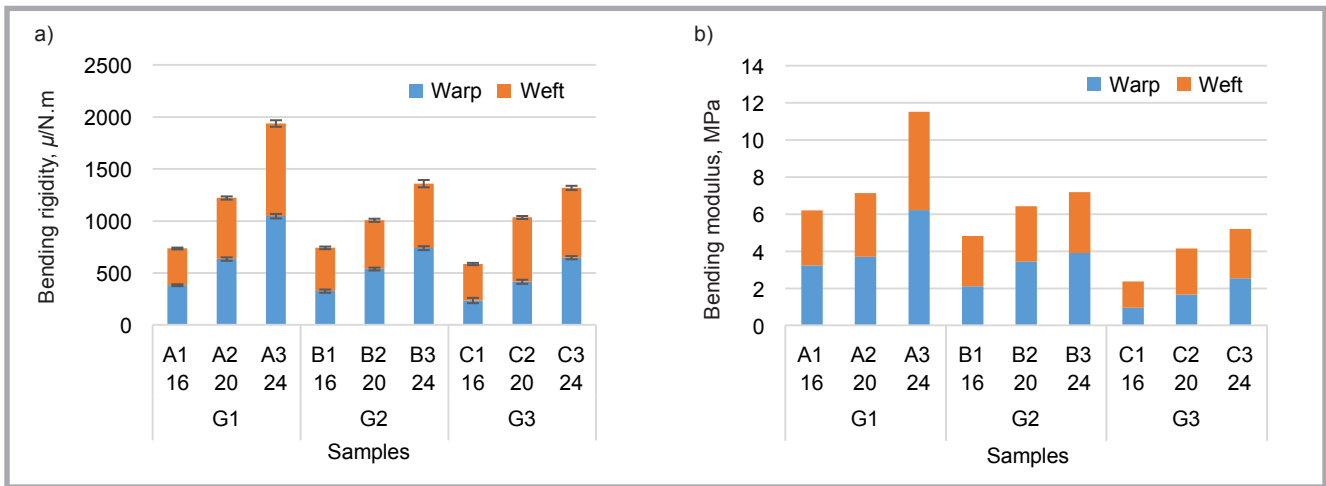


Figure 6. a) Bending rigidity of 3D multilayer fabrics and b) bending modulus of 3D multilayer fabrics.

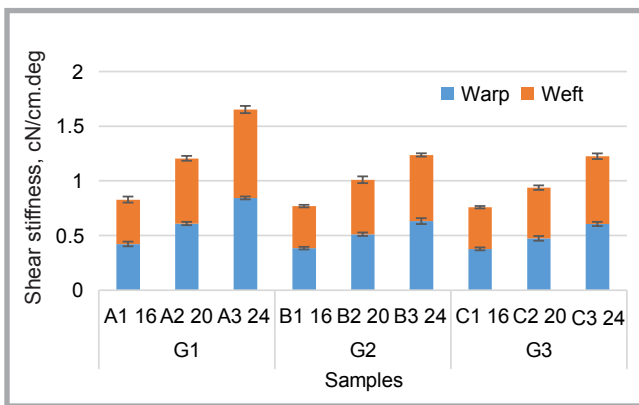


Figure 7. Effect of multilayer structure on shear stiffness.

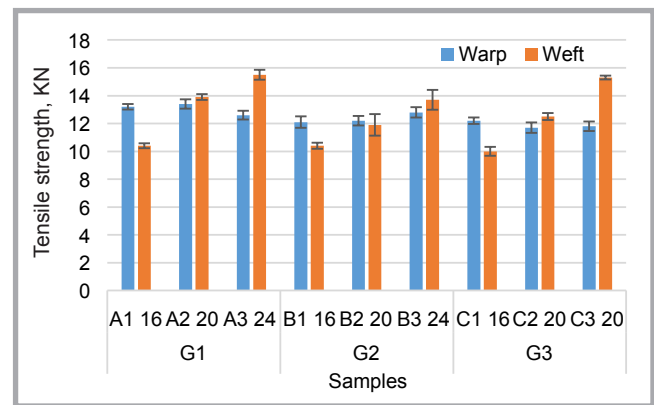


Figure 8. Effect of multilayer structure on tensile strength.

Table 8. Analysis of variance for bending rigidity.

Source	DF	Adj SS	Adj MS	F-value	P-value
Fabric	8	4104386	513048	734.14	0.008
Error	18	12579	699		
Total	26	4116965			

Table 9. Analysis of variance for shear stiffness

Source	DF	Adj SS	Adj MS	F-value	P-value
Fabric	8	2.04498	0.255622	120.68	0.008
Error	18	0.03813	0.002118		
Total	26	2.08311			

Table 10. Analysis of variance for warp tensile strength.

Source	DF	Adj SS	Adj MS	F-value	P-value
Fabric	8	9.0287	1.12859	58.42	0.000
Error	18	0.3477	0.01932		
Total	26	9.3765			

Table 11. Analysis of variance for weft tensile strength.

Source	DF	Adj SS	Adj MS	F-value	P-value
Fabric	8	9.0287	1.12859	58.42	0.000
Error	18	0.3477	0.01932		
Total	26	9.3765			

sign a new flex meter, shown in **Figure 1**. Free image analysis software developed by the National Institute of Health was used to measure the bending length accurately.

The bending rigidity and modulus were evaluated using **Equations (1)** and **(2)**, the results of which are shown in **Figures 6.a** and **6.b**.

It can be inferred from the **Figure 6.a** and **Table 8**, showing  $P \leq 0.05$ , that the fabric structure and pick density both have a significant effect on bending rigidity. If we compare the three groups –  $G_1$ ,  $G_2$  and  $G_3$  for the effect of weave structure, it is evident that the fabric produced with plain weave in all layers possesses higher a bending rigidity and modulus, followed by 1/3 twill and 3/1 rib weaves in the middle layers. All three samples  $A_3$ ,  $B_3$  and  $C_3$  among the groups –  $G_1$ ,  $G_2$  and  $G_3$  present a higher bending rigidity and modulus, which might be due to their higher pick density.

### Effect of structure on shear stiffness

The shear stiffness was measured on a KES FB1 simple shear according to the Kawabata standard. The shear stiffness, which is the slope of the normalised shear force versus the angle curve, is measured between a shear angle of 0.5° and 5°. The mean of the shearing stiffness of the five specimens is shown in **Figure 7**.

It is again evident from **Figure 7** and **Table 9**, showing  $P \leq 0.05$ , that the weave structure of the fabric has a significant effect on shear stiffness. All types of fabrics in group  $G_1$  exhibited higher shear stiffness when compared with specimens from  $G_2$  and  $G_3$  produced with 1/3 twill and 3/1 rib weaves in the middle layers.

The sample produced with higher weft density also presented higher shear stiffness for the same weave design.

### Effect of structure on tensile strength

It was not possible to test the specimens on an MST 20 M dynamometer in our laboratory due to the higher slippage of material, therefore the tensile strength was measured on a LLOYD LR 100 K dynamometer at the company COBRA Europe (specialist in the manufacture of conveyor belts) according to their standard. The mean of the tensile strength for five specimens is recorded in **Table 4** and shown in **Figure 8**.

It can be seen from the results in **Figure 7** and **Tables 10** and **11**, showing  $P \leq 0.05$ , that the weave structure has a significant effect on the tensile strength of the fabric in the warp and weft directions. The warp and weft tensile strength was observed higher for group  $G_1$  of multilayer fabric (plain weave in three layers) as compared with groups  $G_2$  and  $G_3$ , produced with 1/3 twill and 3/1 warp rib in the middle layers.

The effect of the weave structure is more significant along the weft as compared with the warp direction.

Multilayer fabrics  $A_3$ ,  $B_3$  and  $C_3$  exhibited higher tensile strength in the weft direction as compared to the other samples in the three groups, which might be the result of the higher pick density of those fabrics.

## Conclusions

In this study we can conclude that all specimens in group  $G_2$  exhibited higher air permeability and resilience, as shown in **Figure 2** and **3**, when compared with groups  $G_1$  and  $G_3$ . It might be the result of more spaces and the longer diagonal float among the yarns because of the twill weave in the middle layer of the fabrics. All the fabric samples in group  $G_3$ , as shown in **Figure 4**, presented higher compressibility as compared with groups  $G_1$  and  $G_2$ , which might be attributed to the longer straight floats due to the rib weave in the middle layer of these fabrics. The fabric specimens in group  $G_1$ , as shown in **Figure 6.a** and **6.b**, exhibited a higher bending stiffness, shear stiffness and bending modulus when compared with specimens in groups  $G_2$  and  $G_3$ , which might be the result of the higher intersections among yarns in plain weave in the middle layers as compared with twill and rib weaves.

The tensile force in the warp direction for all specimens was comparable because of the same warp density, while it was higher in the weft direction for samples  $A_3$ ,  $B_3$  and  $C_3$ , produced with the highest weft density among the three groups –  $G_1$ ,  $G_2$  and  $G_3$ .

## References

1. Dong Y, Ni Q-Q, Li L, Fu Y. Novel Vapor-Grown Carbon Nanofiber/Epoxy Shape Memory Nanocomposites Prepared via Latex Technology. *Mater Lett*. 2014; 132: 206-9.
2. Nishikawa M, Wakatsuki K, Takeda N. Thermomechanical Experiment and Analysis on Shape Recovery Properties of Shape Memory Polymer Influenced by Fiber Reinforcement. *J Mater Sci*. 2010; 45(14): 3957-60.
3. Turner P, Liu T, Zeng X. Collapse of 3D Orthogonal Woven Carbon Fibre Composites under In-Plane Tension/Compression and Out-Of-Plane Bending. *Compos Struct*. 2016; 142: 286-97.
4. Hart KR, Chia PXL, Sheridan LE, Wetzel ED, Sottos NR, White SR. Mechanisms and Characterization of Impact Damage in 2D and 3D Woven Fiber-Reinforced Composites Part A Applied Science and Manufacturing, 2017.
5. Goda I, Ganghoffer J-F. Construction of First and Second Order Grade Anisotropic Continuum Media for 3D Porous and Textile Composite Structures. *Compos Struct*. 2016; 141: 292-327.
6. Rahali Y, Assidi M, Goda I, Zghal A, Ganghoffer J-F. Computation of the Effective Mechanical Properties Including Nonclassical Moduli of 2.5 D and 3D

Interlocks by Micromechanical Approaches. *Compos Part B Eng*. 2016; 98: 194-212.

7. Rahali Y, Goda I, Ganghoffer J-F. Numerical Identification of Classical and Nonclassical Moduli of 3D Woven Textiles and Analysis of Scale Effects. *Compos Struct*. 2016; 135: 122-39.
8. Elias A, Laurin F, Kaminski M, Gornet L. Experimental and Numerical Investigations of Low Energy/Velocity Impact Damage Generated in 3D Woven Composite with Polymer Matrix. *Compos Struct*. 2017; 159: 228-39.
9. Khokar N. 3D-Weaving and Noobing: Characterization of Interlaced and Non-Interlaced 3D Fabric Forming Principles. Chalmers University of Technology; 1997.
10. Chen X, Taylor LW, Tsai L-J. An Overview on Fabrication of Three-Dimensional Woven Textile Preforms for Composites. *Text Res J*. 2011; 81(9): 932-44.
11. Fukuta K, Miyashita R, Sekiguti J, Nagatsuka Y, Tsuburaya S, Aoki E, et al. Three-Dimensional Fabric, and Method and Loom Construction for the Production Thereof. Google Patents; 1974.
12. Tong L, Mouritz AP, Bannister MK. 3D Fibre Reinforced Polymer Composites. Elsevier; 2002.
13. Chen F, Hodgkinson JM. Impact Behaviour of Composites with Different Fibre Architecture. *Proc Inst Mech Eng Part G J Aerosp Eng*. 2009; 223(7): 1009-17.
14. Brandt J, Drechsler K, Arendts F-J. Mechanical Performance of Composites Based on Various Three-Dimensional Woven-Fibre Preforms. *Compos Sci Technol*. 1996; 56(3): 381-6.
15. Stig F, Hallström S. Assessment of the mechanical properties of a new 3D woven fibre composite material. *Compos Sci Technol*. 2009; 69(11-12): 1686-92.
16. Wang Y, Zhao D. Effect of fabric structures on the mechanical properties of 3-D textile composites. *J Ind Text*. 2006; 35(3): 239-56.
17. Yu B, James Lee L. A Simplified In-Plane Permeability Model for Textile Fabrics. *Polym Compos*. 2000; 21(5): 660-85.
18. Grujicic M, Chittajallu KM, Walsh S. Effect of Shear, Compaction and Nesting on Permeability of the Orthogonal Plain-Weave Fabric Preforms. *Mater Chem Phys*. 2004; 86(2-3): 358-69.
19. Bilisik K. Bending Behavior of Multilayered and Multidirectional Stitched Aramid Woven Fabric Structures. *Text Res J*. 2011; 81(17): 1748-61.
20. Peirce FT. 26 – The “Handle” Of Cloth As A Measurable Quantity. *J Text Inst Trans*. 1930; 21(9): T377-416.
21. Saville BP. Comfort. Phys Test Text Woodhead Publ Ltd, Cambridge, Engl. 1999; 209-43.
22. Bona M. Modern Control Techniques in the Textile Finishing and Making-Up. 1990.

Received 14.01.2020 Reviewed 30.12.2020